Speed Control of Switched Reluctance Motor Drive Powered by A Fuel Cell

Xiang Chen, Meranda Salem, Tuhin Das and Swaminathan Gopalswamy

Abstract— This study presents a speed control design for switched reluctance motor (SRM) drive powered by a fuel cell system. The whole control mechanism consists of a hysteresis current controller to minimize the torque ripple and a P-I speed controller. The control design results are then validated in real-time on a two-node RT-Lab^{TM} platform, together with a fuel cell stack model developed in Emmeskay Inc. It is noted that, although the $P-I$ control is designed based on a low-order simplified model, for simulation purpose, the nonlinear inductance model of an 8/6 SRM is used with classic power chopper.

I. Introduction

Switched Reluctance Motor (SRM) drive has been considered as a possible alternative in variable speed applications because of its obvious advantages[12], [13], [15]: rugged and simple construction, inherent variable speed capability, and ease of control. SRM drive so far has been used in aircraft starter/generator systems, automotive and home appliance applications. SRM drive is also known for their fault tolerant operation as there are no windings or permanent magnets on the rotor, which makes very high-speed operation possible without much concern about the centrifugal forces. In the power chopper side, since the phase windings are connected in series with the upper and lower switches, shoot-through fault does not happen in case that one of the switches is shorted. There are, of course, some disadvantages of SRM drive, such as high level of acoustic noise[4], [6], [7] and torque ripple [15], [18], especially at low operating speed. Therefore, in order for the performance of a switched reluctance motor drive to accommodate different applications, it has to be tailored through appropriate control.

Several drive control methods for SRM have been proposed in literatures in the last decade: sensorless control using a mechanical position sensor[2], [10], fuzzy logic control [3], artificial intelligence control[9], fixed angle control[17], etc. Among them the sensorless control strategy reduces overall cost and dimension of the drive and improves the product reliability, although all other methods have their own pros and cons depending on the principles of operation applied. Ideally, it is desirable to have a drive control scheme which smoothes both the SRM torque and speed and does not require complicated tool to implement it.

In this paper, we investigate a simple speed control design for SRM drive consisting of a hysteresis current control from[5] in the inner loop and a $P-I$ control in the outer loop. The $P-I$ control is designed by ignoring the electrical dynamics in SRM which is much faster than mechanical dynamics. The performance of such control design is then validated by real-time fixed step simulation for a high-order SRM drive model using RT-Lab^{TM} technology from Opal-RT, Inc. In the simulation, it is assumed that the SRM is powered by a fuel cell system, which has been for a long time treated as a potential alternative 'clean' energy source to the current 'dirty' fossil chemical energy source in, for example, automotive industry. This is an interesting combination as a fuel cell plus a motor forms a very generic drivetrain prototype of an electric car. Considering special features of a fuel cell system, the simulation results are very interesting by illustrating how a SRM drive could perform in such as a potential new power system. This research, therefore, actually target on developing potential electric vehicular drivetrain based on fuel cells, which could offer high-energy conversion efficiency and effective energy recovery among other measures. In general, the fuel cell generation system consists of a reformer, a stack and power converter. The power converter converts low voltage dc to ac or high voltage dc. The power converter must have functions to protect the system from output fluctuations reverse currents, and sudden load variations. In this study, a dc/dc converter is used to isolate the fuel cell voltage applied to SRM from any other load that could be powered by the fuel cell system. The ratio of the input voltage to the output voltage for the dc/dc converter used in this research is 5/9. It boosts up the fuel cell voltage from 150v to 270v that is needed to power the SRM. For the purpose of the study in this paper only the fuel cell stack model is included. It is pointed out that the software package of fuel cell model is developed by Emmeskay Inc. It is also noted that the fixed step simulation mechanism in this paper opens a door for future development of hardware-in-the-loop simulation which is very popular nowadays in practices.

This paper is divided into 5 sections. After Introduction, in Section 2, Speed control for SRM drive is presented; in Section 3, fuel cell stack is introduced;

This research is supported in part by NSERC Grant and the technical support by Opal-RT.

Xiang Chen and Meranda Salem are with Department of Electrical and Computer Engineering, University of Windsor, Windsor, Ontario, Canada N9B 3P4. xchen@uwindsor.ca

Tuhin Das and Swaminathan Gopalswamy are with Emmeskay, Inc., 44191 Plymouth Oaks Blvd., Ste. 300, Plymouth, MI 48170 U.S.A.

in Section 4, simulation results are presented for SRM drive control with a fuel cell stack model, while Conclusion can be found in Section 5.

Symbols used in this paper: V_k–the k-th phase voltage; R_k–the k-th phase resistance; i_k–the k-th phase current; $L_a(i_k)$–inductance profile versus current at aligned position; $L_m(i_k)$–inductance profile versus current at midway position; $L_u(i_k)$–inductance profile versus current at unaligned position; ω–SRM speed in rad/sec; θ–SRM shaft angle; $L(i_k, \theta)$–self inductance; T_l–disturbance torque; T_m–SRM electromagnetic torque; I_r–reference current; ω_r–reference speed.

II. Speed Control for SRM Drive

SRM is a salient machine with unequal number of stator and rotor poles[12], [13]. Normally, the ratio of the number of stator poles to rotor poles is 6/4 or 8/6. In an SRM, the reluctance of the magnetic flux path in a given phase changes with rotor movement. The reluctance is maximum when the stator and rotor poles are aligned and minimum when the poles are unaligned. This variation in reluctance reflects in the self-inductance of the respective stator phase. When the stator and rotor poles are aligned, the self-inductance of the stator phase will be maximum and when the poles are unaligned, the self-inductance of the phase will be minimum. In order to have efficient electromechanical energy conversion, the switched reluctance motors are usually designed to operate at high levels of magnetic saturation and hence the air gap length is very small compared to other motors. The magnetic behavior of the steel lamination change with varying levels of saturation and it is reflected in the inductance as well. Thus, the stator phase inductance varies with the instantaneous phase current at any given rotor position. Because of the magnetic saturation, the stator phase inductance at the aligned position varies considerably with the variation in the stator phase current. The unaligned inductance does not vary much mainly because of the large reluctance caused due to the huge air in the flux path. Though the inductance variation with rotor position is trapezoidal in nature, in reality, the edges in the trapezoid are rounded off due to local saturation effects, thus making the inductance variation look more like a distorted sinusoid with a dc offset.

The SRM drive speed control in this paper is divided into two functional units: one is for current control which regulate and smooth the SRM current ripples to make sure the driving torque to achieve the desired drive speed; the other one takes the difference between the drive speed and the reference speed and calculate (through a $P-I$ algorithm) the desired current to be refereed by the current controller as shown in Figure 1.

Note that the equivalent mechanical block includes both SRM rotating part and the mechanical load on the shaft. No disturbance torque is assumed on the shaft.

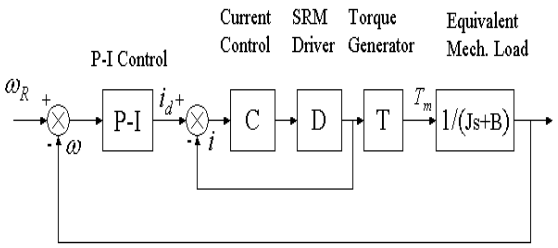

Fig. 1. Block Diagram of SRM Drive Speed Control

For the SRM, an inductance based model[5] of an 8/6 four phases SRM drive is used, which is summarized as follows:

1). The k-th ($k = 1, 2, 3, 4$) phase voltage equation and torque generation equation:

$$V_k = R_k i_k + \Omega^T(\theta)\left(\Lambda(i_k) + i_k \frac{d\Lambda(i_k)}{di_k}\right)\frac{di_k}{dt} + \\ + i_k \omega \frac{d\Omega^T(\theta)}{d\theta}\Lambda(i_k),$$

where $L(i_k, \theta) = \Omega^T(\theta)\Lambda(i_k)$,

$$\Lambda(i_k) = \left[\begin{array}{ccc} L_a(i_k) & L_m(i_k) & L_u(i_k) \end{array}\right]^T,$$

and

$$\Omega^T(\theta) = \left[\begin{array}{c} 0.25 + 0.5\cos(6\theta) + 0.25\cos(12\theta) \\ 0.5 - 0.5\cos(12\theta) \\ 0.25 - 0.5\cos(6\theta) + 0.25\cos(12\theta) \end{array}\right].$$

The torque generation of an SRM is determined by

$$T_m = \sum_{k=1}^{4} \frac{\partial \Omega^T(\theta)}{\partial \theta} \int_0^{i_k} \Lambda(i_k) i_k di_k,$$

2). Mechanical load equations: $T_m - T_l = J\frac{d\omega}{dt} + B\omega$, where J and B are equivalent load inertial and damping, including both SRM rotating part and mechanical load on the shaft.

3). Current control, SRM driver and torque generator: as indicated in the phase voltage-current and torque generation equation, one could expect that current control and SRM driver are complicated. Indeed, it is not a feasible way to conduct SRM drive speed control based on their models. On the other hand, current and drive control are normally conducted by power electronic switch circuits so the electrical processes represented by them are in general much faster than the mechanical process in an SRM. This fact suggests that one may be able to ignore the electrical dynamics for designing $P-I$ speed control design. However, one does need current and drive control in practice to smooth and regulate SRM current/torque ripples. Therefore, the design strategy in this paper is to adopt the hysteresis current control and SRM driver circuits presented in [5] but design the $P-I$ control based

on mechanical load model only. For this account, the circuit control and SRM driver circuits used in the simulation are shown in Figures 2 and 3:

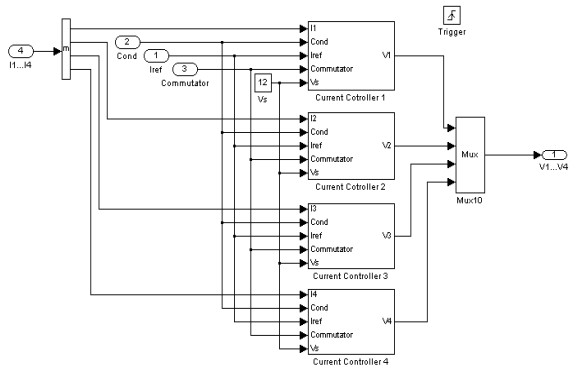

Fig. 2. (Simulation) Circuit of Hysteresis Current Control

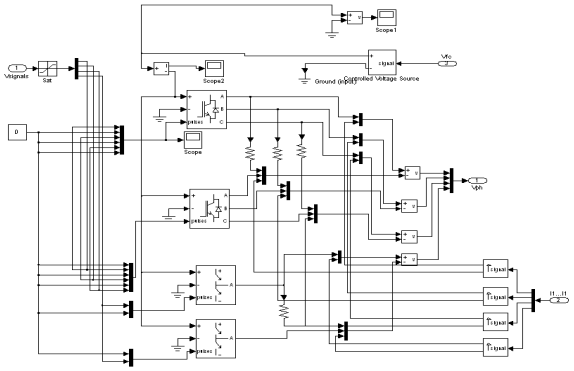

Fig. 3. (Simulation) Circuit of SRM Driver

4). $P-I$ Control Design: The block diagram in Figure 4 is used for $P-I$ control design:

Linearizing the torque generation, an augmented $P-I$ control is obtained as shown in Figure 5. Suppose that $T_m = K_p\delta\omega + K_i\int_0^t \delta\omega dt$, $\delta\omega = \omega_r - \omega$. We have

$$T_m = K_p\delta\omega + K_i\int_0^t \delta\omega dt = J\frac{d\omega}{dt} + B\omega.$$

The Laplace transfer function from $\omega_r(s)$ to $\omega(s)$ can be derived as

$$\frac{\omega(s)}{\omega_r(s)} = \frac{K_p s + K_i}{Js^2 + (K_p + B)s + K_i} = \frac{\frac{K_p}{J}s + \frac{K_i}{J}}{s^2 + \frac{K_p+B}{J}s + \frac{K_i}{J}}$$

The controller parameters K_p and K_i could be designed to achieve a pair of desired poles which satisfy the desired performance requirement. For example, if using the damping ratio ζ and natural frequence ω_n to characterize the poles, then we have $\frac{K_p+B}{J} = 2\zeta\omega_n$, $\frac{K_i}{J} = \omega_n^2$, which solves $K_p = 2J\zeta\omega_n - B$ and $K_i = J\omega_n^2$.

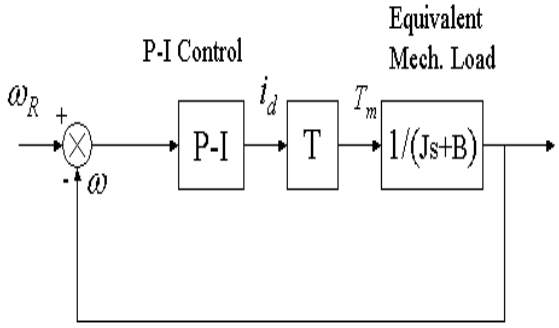

Fig. 4. Block Diagram for $P-I$ Control Design

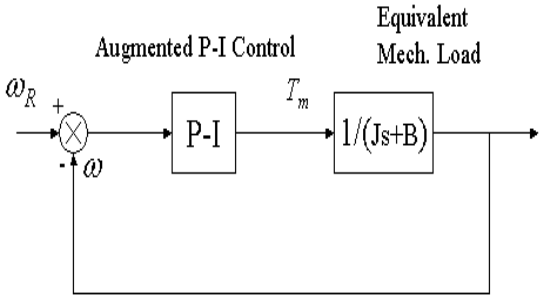

Fig. 5. Block Diagram for Augmented $P-I$ Control Design

III. Fuel Cell Stack

Fuel cell is an electrochemical device that converts the chemical energy of gaseous fuel directly into electricity and is widely regarded as a potential alternative stationary and mobile power source as it reduces the ubiquitous dependence on fossil fuels and thus has significant environmental implication. Fuel cell stack system is under intensive development by several manufacturers, with the Proton Exchange Membrane (PEM) Fuel Cell (also known as the Polymer Electrolyte Membrane Fuel Cell) currently considered to be in a relatively more advanced stage for ground vehicle applications [8]. It is a confirmed fact that there are lot of interests in developing fuel cell powered vehicles from both the government and automobile original equipment manufacturers[11]. In the vehicular application of fuel cell power, transient behavior of is one of the key issues for the success of fuel cell powered vehicles. During the transient process, the fuel cell stack control system is required to maintain optimal temperature, membrane hydration, and partial pressure of the reactants across the membrane in order to avoid degradation of the stack voltage, and thus, maintain high efficiency and extend the life of the stack [1]. There are different types of fuel cells, distinguished mainly by the type of electrolyte used. Different type of fuel cell is suitable for different applications, because of

the differences in characteristics, such as cell material, operating temperature, and fuel diversity. Due to the special feature of fuel cell power system, it is very important to investigate how an SRM drive could perform if it is powered by a fuel cell system, which is presented in the simulation results of this paper.

The transients of fuel cell stack system including the fuel cell controller are modeled in this paper using a software package provided by Emmeskay, Inc., which is shown in Figure 6.

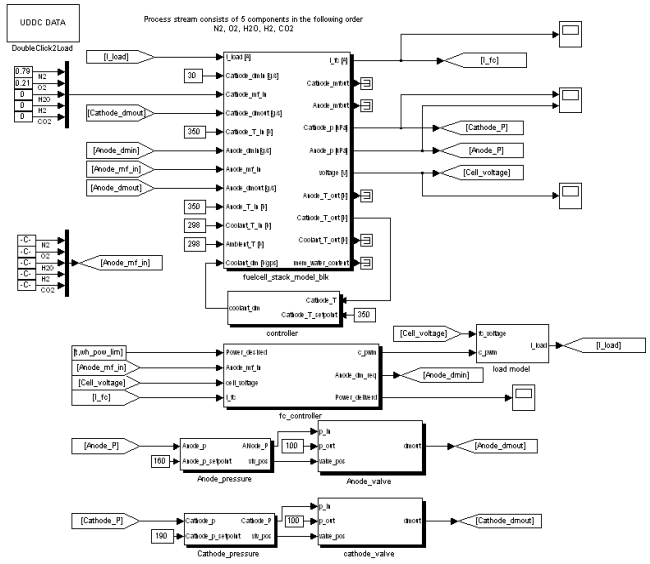

Fig. 6. Block Diagram of Fuel Cell Stack

Emmeskay has developed a lumped-parameter based model of a Proton Exchange Membrane [16], [14] based fuel cell stack. The stack model captures details of pressure dynamics and thermal characteristics of the anode and cathode volumes. A rigorous model of the membrane water balance is included and thermal characteristics of the coolant flow are modeled. Correspondingly, the chemical species concentrations are tracked through the fuel cell stack. The cell voltage computation considers the prominent losses in PEM fuel cells such as activation, ohmic, and concentration losses. The model is parameterized sufficiently to allow testing with a variety of membranes, coolants, catalyst loading, thermal properties, stack geometry, etc. Currently the FC stack is modeled using a Nafion112 membrane, and the FC stack consists of 200 cells, each cell provides approximately 0.8V. In particular, this fuel cell stack model is applied to powering SRM driver and the SRM 4 phase currents are fedback through a current converter(see Figure 7) to control the fuel cell voltage.

At the output of fuel cell voltage, a DC/DC converter (Figure 8) is added to boost up the fuel cell voltage to drive the SRM and to provide isolation between fuel cell and SRM.

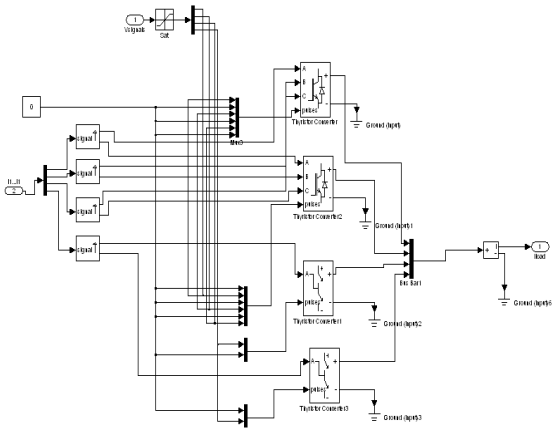

Fig. 7. Simulation Diagram for Current Converter

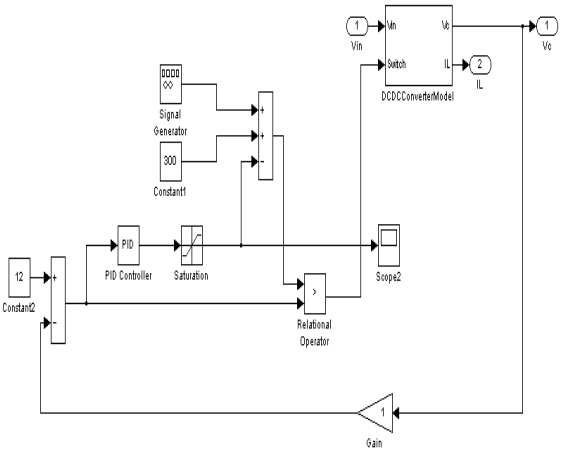

Fig. 8. Simulation Diagram for DC/DC Chopper

IV. Simulation Result

Based on the SRM drive speed control model and the fuel cell stack model presented in previous sections, a real-time simulation is built and operated on a two-node RT-Lab^{TM} platform of Opal-RT Technologies, Inc. For system integration, the following block diagrams are presented: full detail diagram of SRM drive control in Figure 9 and fuel cell stack system in Figure 10. The integrated system is shown in Figure 11.

As shown in the Figure 10, the fuel cell provides voltage through the DC/DC chopper to SRM drive system while the SRM 4 phase currents are fedback through the current converter to regulate the fuel cell voltage. Through these connections, the SRM drive speed control model exchanges data in real time with the fuel cell stack model operating on a two-node RT-Lab^{TM} platform with the SRM drive speed control model on one and the fuel cell stack model on the other. Although the electrical process in SRM drive is ignored when designing the PI-control as stated before, circuit models for the hysteresis current controller and

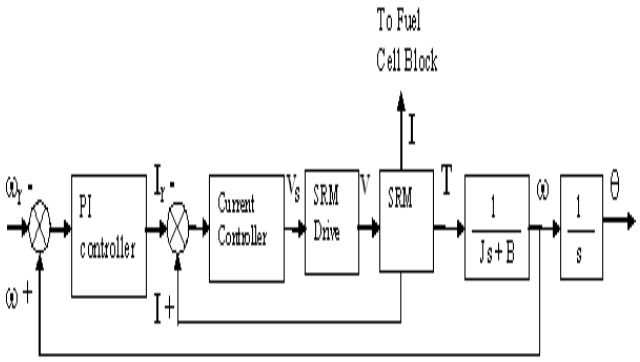

Fig. 9. Full Detail Diagram of SRM Drive Control

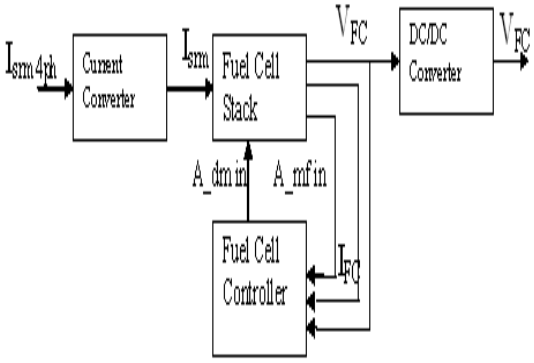

Fig. 10. Block Diagram of A Fuel Cell Stack and Control

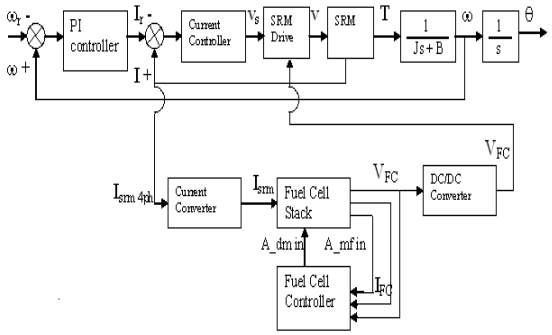

Fig. 11. Real-Time Simulation of Integrated SRM Drive and Fuel Cell Stack

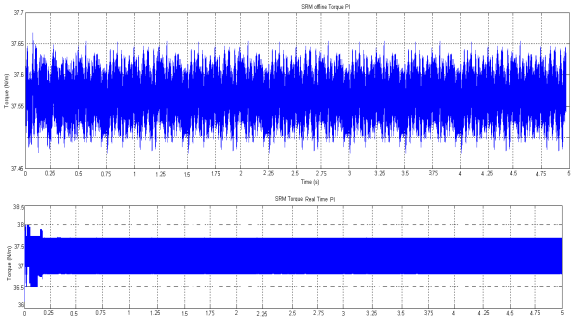

Fig. 12. Off-Line and Real-Time Simulation of SRM Drive Torque

the SRM driver presented in previous section are added when doing simulation. This guarantees that a high-fidelity model is used in simulation to test the validity of the speed control performance.

The real-time simulation is conducted in this paper for an SRM drive with the following specification: rated power $P_{rated} = 90KW$, rated speed $\omega_{rated} = 25,000RPM$, stator/rotor $N_s/N_r = 8/6$, phase $N = 4$, inertial $J = 0.0016kg \times m^2$, damping $B = 0.004N \times m \times sec/rad$.

It is desired that SRM drive possesses $\zeta = 0.7$ and $\omega_n = 400rads/sec$. It can be calculated that, for this case, $K_p = 0.892$ and $K_i = 256$. The real-time simulation results are validated by its off-line (variable step) simulation counterparts as shown in Figures 12 and 13 for SRM torque and speed. As references, both off-line and real-time simulation results of SRM current and fuel cell voltage before and after the DC/DC chopper are also presented (Figure 14, 15 and 16).

Notes on Simulation Results:

1). Although the difference exists in tight ranges between off-line and real-time simulation results, the trends indicate the validity of real-time simulation mechanism to a great extent. It is worth pointing out that this real-time simulation mechanism could be potentially converted into a hardware-in-the-loop simulation to include real devices such as a real fuel cell controller, real SRM drive circuits, a real $P-I$-controller, or even a real SRM itself, depending on what need to be tested.

2). It is noted that, due to the regulating action of $P-I$-controller, both speed and torque yield quite smooth response with no or less ripples.

3). Off-line and real-time results of SRM current are shown in 4 phases.

4). Regulating action of fuel cell control (inside Emmeskay model) yields smooth output voltage which is desired.

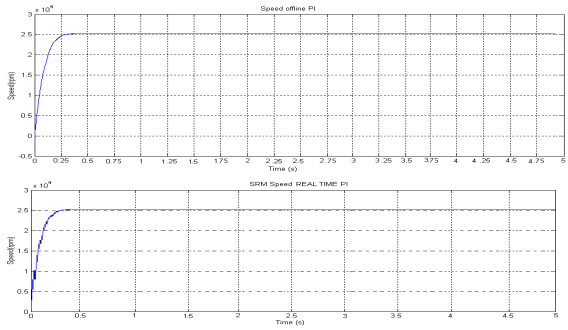

Fig. 13. Off-Line and Real-Time Simulation of SRM Drive Speed

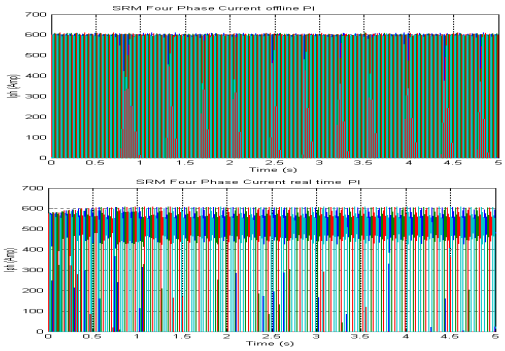

Fig. 14. Off-Line and Real-Time Simulation of SRM Current

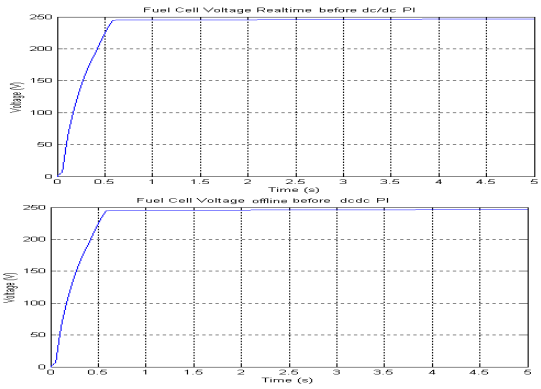

Fig. 15. Off-Line and Real-Time Simulation of Fuel Cell Voltage before DC/DC Chopper

V. Conclusion

In this paper, a simple and effective speed control design of SRM drive is proposed consisting of a hysteresis current control and a $P-I$ regulator. The $P-I$ control is designed based on a low-order mechanical load model ignoring the electrical dynamics in SRM. This speed control design is validated for a full detail SRM drive model powered by a fuel cell system in a real-time simulation conducted on a two-node RT-Lab^{TM} platform. Both off-line variable step and real-time fixed step simulation results are presented for validation purpose. The results show the promising performance of the proposed control design. The results also indicate a low cost feasible real-time simulation mechanism to support both fuel cell and motor drive control related research and development work. It is noted that this mechanism could be potentially converted into a hardware-in-the-loop simulation to include real devices.

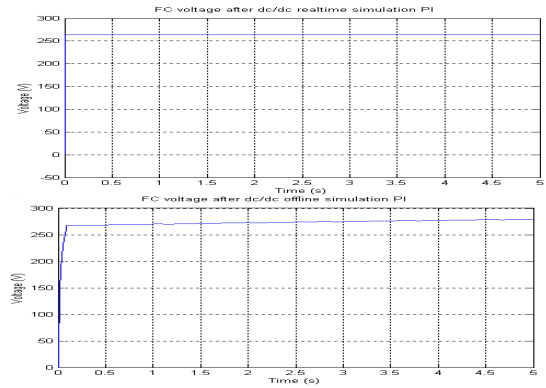

Fig. 16. Off-Line and Real-Time Simulation of Fuel Cell Voltage after DC/DC Chopper

References

[1] Appleby, A. J. and Foulkes, F.R., Fuel Cell Handbook, Van Nostrand Reinhold, New York, 1989.

[2] Bose, B.K., Miller, T., Szczensny, P.M., and Bicknell, W. H., "Microcomputer Control of Switched Reluctance Motor", IEEE Trans. on Industry Applications, Vol. IA-2, pp.708-715, 1986.

[3] Rodrigues, M. G., Suemitsu, W. I., Branco, P., Dente, J.A., and Rolim, L.G.B."Fuzzy logic control of a switched reluctance motor", Proc. of the IEEE International Symposium on Industrial Electronics (ISIE '97), Vol. 2, pp. 527-531, 1997.

[4] Cameron, D. E., Lang, J.H. and Umans, S.D., "The Origin and Reduction of Acoustic Noise in Doubly Salient Variable Reluctance Motor", IEEE Trans. on Industry Applications, Vol. IA-28, No. 6, pp. 1250-1255, 1992.

[5] Ehsani, M. and Abourida, S., "Design, Analysis and Control of Electrical Motor Drives Using Hardware-in-the-Loop Simulation", Opal-RT Workshop, Livonia, Michigan, November 4-5th, 2003.

[6] Fahimi, B., Control of Vibration in Switched Reluctance Motor Drives, Ph.D. Dissertation, Texas A&M University, 1999.

[7] Fahimi, B., Suresh, G., and Ehsani, M., "Design Considerations of Switched Reluctance Motors: Vibration and Control Issues", IEEE Industry Application Society Annual Meeting, Phoenix, 1999.

[8] Fronk, M.H., Wetter, D. L., Masten, D. A. and Bosco, A., "PEM Fuel Cell System Solutions for Transportation". SAE Paper #2000-01-0373, 2000

[9] Henriques, L.O.A.P., Rolim, L.G.B., Suemitsu, W.I., Branco, P.J.C., and Dente, J.A.,"Torque ripple minimization in a switched reluctance drive by neuro-fuzzy compensation", IEEE Trans. on Magnetics, Vol. 36 , Iss. 5, pp. 3592-3594, 2000.

[10] Hossain, S.A., Husain, I., Klode, H., Lequesne, B., Omekanda, A.M., and Gopalakrishnan, S., "Four-quadrant and zero-speed sensorless control of a switched reluctance motor", IEEE Trans. on Industry Applications, Vol. 39, Issue 5, pp.1343-1349, 2003.

[11] Jost, K., "Fuel Cell Concepts and Technology", Automotive Engineering International, March, 2000.

[12] Lawrenson, P.J., Stephenson, J. M., Blenkinsop, P.T., Corda, J., and Fulton, N.N., "Variable-Speed Switched Reluctance Motors", Proc. IEE, Vol.127, Part B, No.4, pp. 253-265, July, 1980.

[13] Miller, T. J. E., Switched Reluctance Motor and Their Control, Magna Physics Publishing and Oxford Science Publications, London, 1993.

[14] Fronk, M. H., Wetter, D. L., Masten, D. A. and Bosco, A., "PEM fuel cell system solutions for transportation", SAE Paper 2000-01-0373.

[15] Moreira, J., "Torque Ripple Minimization in Switched Reluctance Motors via Bi-cubic Spline Interpolation", Proc. IEEE PESC Conference, pp. 851- 856, 1992.

[16] Pukrushpan, J. T., Modeling and Control of Fuel Cell Systems and Fuel Processors, Ph.D. dissertation, University of Michigan, 2003.

[17] Sharma, V. K., Chandra, A. and Haddad, K. E., "Performance Simulation of SRM Drive System Operating with Fixed Angle Control Scheme", Proc. Electrimacs, 2002.

[18] Wallace, R., Taylor, D.G., "Three-phase Switched Reluctance Motor Design to Reduce Torque Ripple", Proc. International Conference on Electrical Machines, pp. 783-787, 1990.